IOP Conf. Series: Journal of Physics: Conf. Series **796** (2017) 012026 doi:10.1088/1742-6596/796/1/012026

Temperature field for radiative tomato peeling

G Cuccurullo and L Giordano
Department of Industrial Engineering, University of Salerno,
Via Giovanni Paolo II 132, 84084 Fisciano (SA), Italy

E-mail: gcuccurullo@unisa.it

Abstract. Nowadays peeling of tomatoes is performed by using steam or lye, which are expensive and polluting techniques, thus sustainable alternatives are searched for dry peeling and, among that, radiative heating seems to be a fairly promising method. This paper aims to speed up the prediction of surface temperatures useful for realizing dry-peeling, thus a 1D-analytical model for the unsteady temperature field in a rotating tomato exposed to a radiative heating source is presented. Since only short times are of interest for the problem at hand, the model involves a semi-infinite slab cooled by convective heat transfer while heated by a pulsating heat source. The model being linear, the solution is derived following the Laplace Transform method. A 3D finite element model of the rotating tomato is introduced as well in order to validate the analytical solution. A satisfactory agreement is attained. Therefore, two different ways to predict the onset of the peeling conditions are available which can be of help for proper design of peeling plants. Particular attention is paid to study surface temperature uniformity, that being a critical parameter for realizing an easy tomato peeling.

1. Introduction

Nowadays, peeling of tomatoes is performed by using steam or lye, which are expensive and polluting techniques. In this connection, interest in radiative heating as means of sustainable peel removal is growing among the scientists, [1-5]. In facts, after a suitable warming up, loosened skin can be easily removed by mechanical pinch rollers. Thus, predicting the thermal response of the tomato during the radiative dry peeling process can lead to good peeling performance and, in addition, it can be of help in designing a suitable radiative heating system, ensuring high quality of peeled tomatoes and energy saving.

A typical configuration realized in industrial plants for tomatoes skin heating adopts a matrix of infrared emitters. The latter illuminates only one side of the target tomatoes which lay on a conveyor system. Since the target is rotating during the transportation, on average, heat is transferred all over the surface of the tomato, [6]. Computational simulation is usually adopted to describe such a process assuming a radiative opaque behaviour for the tomato, [3-4]. On the other hand, several studies are based on radiative volumetric absorption due to the penetration of infrared (IR) radiant energy at a food surface and, consequently, they deal with semi-empirical exponentially decaying models with a finite penetration depth [7-9].

In this context, the novelty herein presented takes into account the effect of the tomato rotating speed both by numerical and analytical point of view. Formerly, a finite element code, i.e. Comsol Multiphysics, is employed to study a 3D model of the rotating tomato; the shape of the target tomato is suitably adjusted by means of a parametric representation, [3], while radiative behaviour is assumed grey and diffuse. A ceramic emitter acting as heat source is conveniently modelled as well. Correspondingly, an analytical model is introduced which involves a semi-infinite slab cooled by

convective heat transfer and heated by a pulsating heat source; the latter was described as the positive half wave of a sinusoidal function. The proposed analytical solution shows a pretty good agreement with the corresponding numerical model, until the kernel of the tomato remains at the initial temperature. Thus, an easy to handle model for predicting the onset of the peeling conditions is actually available. However, the numerical solution is required wishing to recover a value for the rotational velocity enabling to get the desired uniformity degree for the surface temperature.

2. Basic equations

In the context of industrial tomato processing, successful peel separation requires the surface temperature to attain values as high as 100°C in a very short warming up period, typically no more than 60 s. Assuming water thermophysical properties apply for tomato, it is easy to check that the penetration depth is confined to really few millimeters under the tomato skin. Such consideration suggests to model the tomato as a semi-infinite body subjected to uniform radiative heating. On the other hand, wishing a more detailed description including spatial disuniformities, a numerical scheme is required which accounts for the irregular geometry of tomatoes.

2.1. Analytical solution

Rapid processing determines only surface peripheral warming up. Thus, the tomato under test is modelled as a purely conductive opaque-to-radiation semi-infinite body with constant thermal properties. Latent heat transfer is neglected as well. Considering that surface temperatures of the infrared heaters are much greater than the target ones, a II-type boundary condition is considered for including radiative IR heating. Tomato rotation around its main axis is accounted for by introducing a sinusoidal pulsating heat source. The latter is described as the positive half wave of a sinusoidal function. In addition, the boundary condition on the wall is supplemented by heat transfer linearly depending on wall temperature, with a constant heat transfer coefficient.

Under such assumptions, the dimensionless energy balance and the related boundary conditions lead to a linear problem:

$$\begin{cases} \dfrac{\partial^2\theta}{\partial\xi^2} = \dfrac{\partial\theta}{\partial\tau} \\ -\left.\dfrac{\partial\theta}{\partial\xi}\right|_{\xi=0} = \sin(\tau)\dfrac{\mathrm{sign}[\sin(\tau)]+1}{2} - Bi\,\theta \\ \theta(\xi\to\infty,\tau) = 0 \\ \theta(\xi,\tau=0) = 0 \end{cases} \tag{1}$$

where $\theta=(T-T_f)/\Delta T_{ref}$ is the temperature, T_f representing both the surrounding and the initial temperature; the group $\Delta T_{ref} = \dot{q}_0\, x_{ref}/k$ is a reference temperature difference related to the peak amplitude of the wall heat flux, $\dot{q}_0$, and to a reference length $x_{ref} = (\alpha\, t_{ref})^{1/2}$, k and α being the tomato thermal conductivity and diffusivity; the reference time, $t_{ref} = \Omega^{-1}$, was chosen such as the dimensionless time resulted $\tau = \Omega\, t$, Ω being the angular velocity of the source. The dimensionless space variable was defined such as $\xi = x/x_{ref}$ and, finally, $Bi = h\, x_{ref}/k$ is the Biot number. The function sign(sin(τ)) is a two-valued function switching each half period between zero or one.

Since the problem is linear, the solution can be sought as the sum of two partial solutions, θ_1 and θ_2, each one affected by a single non-homogeneity arising from the boundary condition at the wall; the

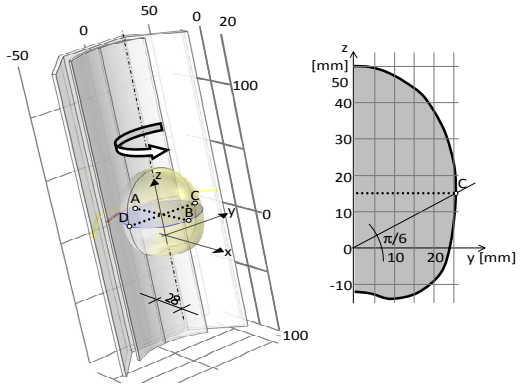

Figure 1. Schematic of the model.

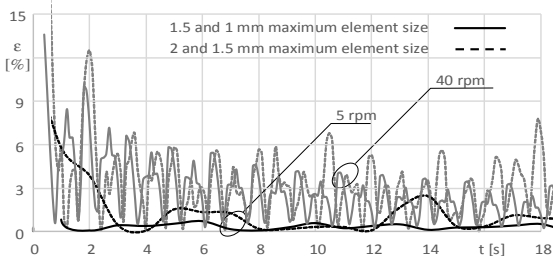

Figure 2. Mesh analysis.

former is due to the heating source and the latter by the cooling surroundings. Then, the two partial solutions have to satisfy two distinct problems derived by the basic one:

$$\begin{cases} \dfrac{\partial^2\theta_1}{\partial\xi^2}=\dfrac{\partial\theta_1}{\partial\tau} \\ \left.\dfrac{\partial\theta_1}{\partial\xi}\right|_{\xi=0}=-\sin(\tau)\dfrac{\text{sign}[\sin(\tau)]+1}{2} \\ \theta_1(\xi\to\infty,\tau)=0 \\ \theta_1(\xi,\tau=0)=0 \end{cases} \qquad \begin{cases} \dfrac{\partial^2\theta_2}{\partial\xi^2}=\dfrac{\partial\theta_2}{\partial\tau} \\ \left.\dfrac{\partial\theta_2}{\partial\xi}\right|_{\xi=0}=Bi\,\theta_2 \\ \theta_2(\xi\to\infty,\tau)=0 \\ \theta_2(\xi,\tau=0)=0 \end{cases} \tag{2}$$

The θ_1-problem is solved in a closed form by the Laplace transform method, while the latter is classically found in literature, see for instance [10]. For such a reason, in what follows, only radiative heat transfer will be dealt with to compare numerical and analytical results without affecting the meaning of the present analysis. After some manipulation, the solution to the first problem is cast as:

$$\theta_1(\xi,\tau)=\int_0^{\tau}\left(-\frac{e^{-\frac{\xi^2}{4\cdot(\tau-y)}}}{\sqrt{\pi}\cdot\sqrt{\tau-y}}\right)\cdot\left(-\sin(y)\cdot\frac{\text{sign}[\sin(y)]+1}{2}\right)\cdot dy=\sum_{k=0}^{n(\tau)-1}(-1)^k\,z_k(\xi,\tau) \tag{3}$$

with $n=\tau/\pi$, if τ/π is an integer otherwise $n=\text{int}(\tau/\pi)+1$ and

$$\begin{aligned} z_k(\xi,\tau)=&-\frac{1}{2\sqrt{2}}\left(e^{-\frac{\xi}{\sqrt{2}}}F_p(\xi_m)\,\text{erfc}\left(\frac{-\sqrt{2}\tau_r+\xi}{2\sqrt{\tau_r}}\right)+e^{\frac{\xi}{\sqrt{2}}}\,\text{erfc}\left(\frac{\sqrt{2}\tau_r+\xi}{2\sqrt{\tau_r}}\right)F_m(\xi_p)\right)+\\ &+\frac{1}{\sqrt{\pi}\sqrt{2}}e^{-\frac{\xi^2+2\tau_r^2}{4\tau_r}}\left(F_c\left(\frac{-\sqrt{2}\tau_r+\xi}{2\sqrt{\tau_r}},\frac{\sqrt{\tau_r}}{\sqrt{2}}\right)F_m(\xi_m)+F_c\left(\frac{\sqrt{2}\tau_r+\xi}{2\sqrt{\tau_r}},\frac{\sqrt{\tau_r}}{\sqrt{2}}\right)F_p(\xi_p)\right)+\\ &+\frac{1}{\sqrt{\pi}\sqrt{2}}e^{-\frac{\xi^2+2\tau_r^2}{4\tau_r}}\left(F_s\left(\frac{-\sqrt{2}\tau_r+\xi}{2\sqrt{\tau_r}},-\frac{\sqrt{\tau_r}}{\sqrt{2}}\right)F_p(\xi_m)+F_s\left(\frac{\sqrt{2}\tau_r+\xi}{2\sqrt{\tau_r}},-\frac{\sqrt{\tau_r}}{\sqrt{2}}\right)F_m(\xi_p)\right) \end{aligned} \tag{4}$$

where $\xi_m=-\tau+\xi/\sqrt{2}$, $\xi_p=\tau+\xi/\sqrt{2}$, $\tau_r=\tau-k\,\pi$; the functions F_c, F_s, F_m and F_p are:

$$F_c(a,b)=\int_0^b u^2\cos(2au)du\ ;\ F_s(a,b)=\int_0^b u^2\sin(2au)du\ ; \tag{5}$$

$$F_p(z)=\cos(z)+\sin(z);\ F_m(z)=\sin(z)-\cos(z) \tag{6}$$

The analytical solution was validated in comparison with the corresponding numerical solution obtained by solving a finite element scheme. Moreover, the accuracy of the solution was also verified with reference to the limiting case of a simple sinusoidal source and checking that it fully recovers the first function of the z_k succession.

2.2. Numerical solution

As witnessed by the leading papers by Pan [3-4], the numerical approach allows a quite satisfactory description of the problem at hand, provided that spatial discretization is performed with care as grid dispersion may arise [6]. On the other hand, numerical modelling may be subjected to long execution times, depending on the evaluation of view factors, thus the hemicube approach is suggested, [11]. A schematic representation of the geometry under study is reported in Figure 1. The heating source consists in an infrared emitter coupled to a polished surface for reflecting radiation which illuminates the tomato from one side. The tomato rotates with a prescribed angular velocity around its main axis which is parallel to the IR emitter. Such configuration should possibly resemble a typical industrial setup. The average surface temperature of the emitter is assumed to be 800°C, a value complying to IR emitters standard performance. Tomato is assumed to be a diffuse gray emitter with a surface absorptivity of 95% [3], while air in the enclosure is assumed as a non-participating medium. Latent loss from tomato surface is neglected since it corresponds to less than 2 or 3 % of the total heat loss, due to the shortness of the heating period, [2].

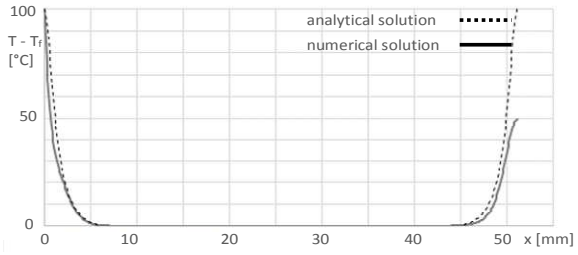

Figure 3a. Temperature profiles along the path AB for 5 after 18 s.

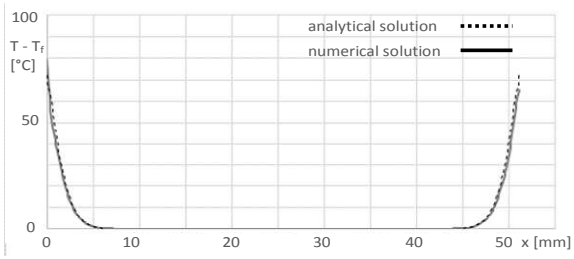

Figure 3b. Temperature profiles along the path AB for 40 rpm after 18 s.

Under the above assumptions, a 3D FEM model was developed by employing the commercial code COMSOL v4.3 [12]. The numerical model determines the unsteady temperature distribution for the rotating tomato by further considering constant flow properties. The computational domain of the tomato was generated based on two-dimensional axisymmetric parametric profile after Li et al., [1]; the related dimensionless shape coefficients were sought as: a = 31 mm, b = 24 mm, c_1 = 0.24, c_2 = 0.38, that identifying a medium size tomato.

The tomato computational domain was discretized using unstructured tetrahedral grid elements. Having in mind to suitably reduce computational burdens, special care was devoted in choosing the mesh size [11]. A mesh convergence study was performed to confirm that results are independent of mesh size during the warming up period, which represents the time needed for the averaged surface temperature to recover the set point value ($T_{objective}$). In practice, such a value is usually selected to be 90°C, which is known to be useful for peeling. The corresponding warming up period turns out to be about 18 seconds. First, a mesh using the fewest, reasonable number of elements was created; the mesh density, expressed in terms of maximum element size, was increased until a satisfactory independence of an objective function by the mesh itself was obtained. The objective function was chosen to be the percentage relative variation of the temperature history, $\varepsilon = (T_{last\text{-}mesh} - T_{previous\text{-}mesh})/ T_{last\text{-}mesh}$, evaluated at the point "C" evidenced in Figure 1. On the above basis, plots of Figure 2 were realized by comparing the objective function evaluated for 2 and 1.5 mm maximum element size, dashed-curves, and for 1.5

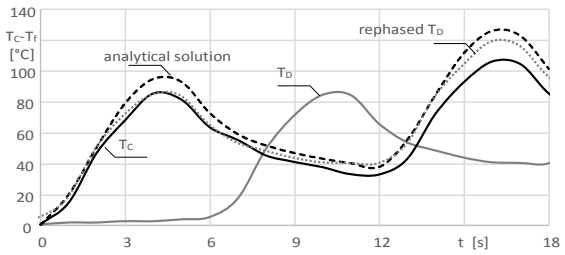

Figure 4a. Temperature – time history of selected points for 5 rpm.

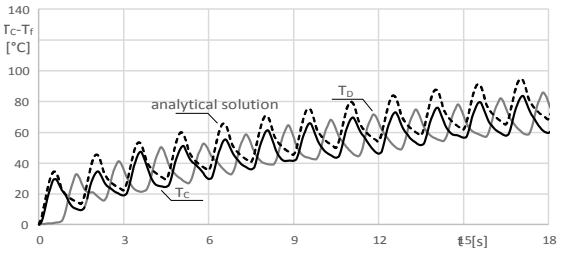

Figure 4b. Temperature – time history of selected points for 40 rpm.

and 1 mm, continuous-curves, for two selected angular velocities, i.e. 5 and 40 rpm. For the lowest angular rotation, results are practically independent of the mesh, while the objective function keeps on fluctuating with double frequency with respect to the source pulsations; in facts, the maximum variations pop up in correspondence of the temperature relative extrema. The same behavior features the highest speed for which, as expected, the objective function attains higher values, even though it becomes regular and contained within the 4% after 9 s for the case related to the finer meshes.

3. Results

3.1. Temperature field

Numerical temperature profiles and the corresponding analytical ones along the path AB during the warming up period are compared in Figure 3 a, b; the points A and B are diametrically opposed and are positioned on the circumference experiencing the maximum wall heat flux, identified by the zenith angle equal to $\pi/6$ in the *yz*-plane from *y*-axis. The analytical solution is drawn by assigning to the parameter $\dot{q}_0$ the average value of the wall heat flux over the whole tomato surface as resulting from the numerical solution at the initial time. A first sign about the ability of the semi-infinite model to describe the problem at hand is witnessed by the appropriate estimate for the penetration depth: it turns out to be $(\alpha t)^{1/2} = 2$ mm, which is much lower than the tomato average radius after 18 s; moreover, such a value is consistent with the corresponding numerical one, as evident by both plots of Figures 3.

Two occurrences are useful in order to assess that the more the angular velocity increases the more suitable is the semi-infinite model; the former consideration consists in observing that the root mean square errors between the numerical and the corresponding analytical plots turn out to be 7 and 1.5 °C for 5 and 40 rpm, respectively; in addition, the magnitudes of the tangential component of the wall heat flux are contained within 1% and 0.2 % of the normal component for 5 and 40 rpm, respectively. Thus, it can be argued that, actually, unidimensional heat transfer takes place.

The temperature-time histories of the points initially positioned in C and D are reported in Figures 4 for two selected angular velocities, i.e. 5 and 40 rpm, and for both the analytical and numerical solutions. For a fixed speed, the numerically evaluated temperature history of the point C exhibits a steep increase because it moves toward the heating source, while the point D temperature history starts with a zero-slope tangent because its exposition to the source is delayed for one half period. Then, temperatures start to fluctuate periodically that depending on the angular velocity in use while their time-average temperature increases.

However, if point D is returned to being in phase with point C, see the dotted curve in Figure 4a, the two related profiles seem to collapse into a single one within an average relative error of 10.2% in the warming up period. With increasing the angular velocity, the amplitude of temperature fluctuations decreases, Figure 4b, because the wall heat flux is more uniformly distributed along a fixed time-interval, the overall incoming energy being the same. In this case, the average relative error between the two rephased profiles lowers to 5.0 %. This occurrence suggests that profiles individuated at different azimuthal angles lose their individuality as much as the frequency increases, thus enabling the use of the semi-infinite model, dashed line in Figures 4.

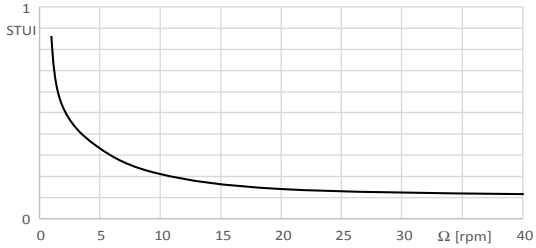

Figure 5. STUI as function of angular velocity after 18 s

It should be emphasized that, for both the rotation speeds, the periodic steady-state response is far from being recovered, thus the sustained solution is not-useful for the specific context at hand.

3.2. Evaluation of surface temperature uniformity

Rapid and uniform surface heating is required to realize an effective IR dry-peeling process, [14-15]. In fact, uneven temperature distributions in tomato surface may determine, in turn, inhomogeneous peeling or product damage. The presence of hot spots can cause deterioration in textural quality and loss in nutritional value of the peeled products, whereas cold spots prevent peel removal. The availability of the numerical scheme allows to study the spatial and temporal temperature uniformity while varying the angular velocity of the sample under test. For such a purpose, a temperature uniformity surface index was introduced which is defined as:

$$STUI = \frac{1}{T_{objective} - T_f} \cdot \sqrt{\frac{\iint \left(T - T_{average}\right)^2 dA}{A}} \tag{7}$$

the area A being the tomato exposed surface.

The STUI turns out to depend on time and angular velocity and is represented in Figure 5 for t = 18 s. For low rotation speeds, increasing the angular velocity rapidly improves tomato temperature uniformity whereas the STUI is less sensitive with increasing the angular velocity. From the industrial point of view, such a behavior can suggest how to suitably select a proper angular velocity featuring the tomato conveyance system.

4. Conclusions

Having in mind the typical warming up serving as preparation for radiative tomato peeling, an analytical 1D unsteady heat transfer model was developed. The solution was compared with a 3D model for the problem at hand showing a fair agreement provided that the typical IR dry-peeling conditions are realized. The availability of both analytical and finite element models can be a starting step to gain insight into the rapid surface heating characteristics of IR radiation in the tomato dry-peeling process.

References

[1] Li X, Pan Z, Upadhyaya S K, Atungulu G G & Delwiche M 2011 Three-dimensional geometric modeling of processing tomatoes, *Transactions of the ASABE* **54** 2287–2296.

[2] Li X 2012 *A study of infrared heating technology for tomato peeling: Process characterization and modeling*, Ph.D. Dissertation (Department of Biological and Agricultural Engineering, University of California at Davis, Davis, CA, USA).

[3] Li X, Pan Z 2014 Dry peeling of Tomato by Infrared Radiative Heating: Part I. Model Development, *Food Bioprocess Technol* **7** 1996–2004.

[4] Li X, Pan Z 2014 Dry peeling of tomato by infrared radiative heating: Part II. Model validation and sensitivity analysis, *Food and Bioprocess Technology* **7** 2005–2013.

[5] Rock C, Yang W, Goodrich-Schneider R & Feng H 2011 Conventional and alternative methods for tomato peeling, *Food Engineering Reviews*, **4** 1–15.

[6] Pan Z, Li X, Khir R, El-Mashad H M, Atungulu G G, McHugh T H., Delwiche M 2015 A pilot scale electrical infrared dry-peeling system for tomatoes: Design and performance evaluation, *Biosystems engineering* **137**, 1-8.
[7] Datta A, Ni H 2002 Infrared and hot-air-assisted microwave heating of foods for control of surface moisture, *Journal of Food Engineering*, **51** 355–364.
[8] Prakash B 2012, *Mathematical modeling of moisture movement within a rice kernel during convective and infrared drying*, Ph.D. Dissertation (Department of Biological and Agricultural Engineering, University of California at Davis, Davis, CA, USA).
[9] Trivittayasil V, Tanaka F, Uchino T 2011 Investigation of deactivation of mold conidia by infrared heating in a model-based approach, *Journal of Food Engineering*, **104** 565–570.
[10] Carslaw H S, Jaeger J C 1959 *Conduction of Heat Solids* 2/E (Oxford University Press).
[11] Howell J R, Siegel R, Menguc M P 2010 Thermal radiation heat transfer 5/E (New York: Taylor and Francis).
[12] COMSOL Multiphysics Version 4.3a User Guide, October 2012.
[13] Cuccurullo G, Giordano L and Viccione G 2013 An Analytical approximation for continuous flow microwave heating of liquids, *Advances in Mechanical Engineering*, **2013**
[14] Geedipalli S, Rakesh V, Datta A 2007 Modeling the heating uniformity contributed by a rotating turntable in microwave ovens, *Journal of Food Engineering*, **82** 359–368.
[15] Tanaka F, Verboven P, Scheerlinck N, Morita K, Iwasaki K, Nicola B 2007 Investigation of far infrared radiation heating as an alternative technique for surface decontamination of strawberry, *Journal of Food Engineering*, **79** 445–452.